iJRASET
International Journal For Research in
Applied Science and Engineering Technology

INTERNATIONAL JOURNAL FOR RESEARCH

IN APPLIED SCIENCE & ENGINEERING TECHNOLOGY

Volume: 11 Issue: I Month of publication: January 2023

DOI: https://doi.org/10.22214/ijraset.2023.48777

Remote Sensing Image-Based Analysis of the Urban Heat Island Effect in Relation to the Normalized Difference Vegetation Index (NDVI): A Case Study of Patna Municipal Corporation

Avinash Yadav[1], Ravish Kumar[2], Sneha Swarup[3]
[1]*Master of Urban & Regional Planning,* [2,3]*Assistant Professor*
[1,2]*Department of Architecture & Planning, National Institute of Technology, Patna, Bihar, India*
[3]*Department of Geography, Swami Sahjanand college, Jehanabad, Bihar, India*

Abstract: The consequences of population growth and urbanization on the urban environment, climate, and water supply have caused a wide range of issues. As a result of the rapid urbanization process, vegetation covers are being converted by impervious and dry concrete covers. This has led to the growth of "heat islands," where urban areas experience warmer temperatures than the areas surrounding them. Urban Heat Island (UHI) is a human-caused environmental phenomenon that has a wide range of impacts on city dwellers, including changing the vegetation cover and its usage, which alters the thermal energy flow and raises surface and air temperatures. Such heat islands have far-reaching impacts for cities, the most significant of which is an increase in the expense of maintaining a safe living and working environment. The major objective of this study is to examine multi-temporal Land Surface Temperature (LST)/Urban Heat Island (UHI) and Normalized Difference Vegetation Index (NDVI) in the Patna Municipal Corporation (PMC) from 1990 to 2022. The Landsat satellite data sets for the years 1990, 2001, 2011, and 2022 have used to investigate the impact of UHI/LST in relation to NDVI in the study area. The most significant change has been observed in vegetation cover (NDVI), which has declined compared to other types of land use land cover. According to the study, built-up area and barren land have high temperatures, whereas vegetated covers and water bodies have lower temperatures. The LST of some portion of study area is high due to the high population density and high percentage of built-up and concrete cover. The LST over the study area has risen on average by 6.88 °C between 1990 and 2022. The regression line provided a conclusive answer, demonstrating a strong negative relationship between the normalized difference vegetation index (NDVI) and UHI of PMC. According to the findings of this study, a major transition has occurred in PMC in terms of a decline in NDVI due to a rapid growth in urban expansion, and other infrastructure projects. To study urban climate and interactions between people and the environment, land surface temperature (LST) variations within cities are of utmost importance in respect to ascertain the LST/Urban Heat Island (UHI) effect and NDVI variations in PMC. While developing urbanization, the environmental impact must be taken into account.

Keywords: UHI effect, LST, NDVI, and Correlation between NDVI and LST

I. INTRODUCTION

The world's population has been steadily increasing, and people are migrating from rural to urban areas. As a result, urbanization has had an impact on the environment, has been the root cause of climate change, and has resulted in environmental degradation and health hazards. As a result of the rapid urbanization process, green urban areas are being replaced by impermeable and dry concrete surfaces (Anindita Bhattacharjee, 2022). The ecosystem of the world has recently experienced climatic change. According to scientists, global temperatures will continue to increase for decades due to greenhouse gases emitted by human activities such as the usage of air conditioning for thermal comfort. Global climate change is degrading the urban sustainability situation of people who reside in cities and their environs for a variety of reasons, one of which being increased urbanization in major cities (Marando et al., 2022). According to the United Nations, the world's population will grow by 2 billion over the next 30 years, from 7.7 billion now to 9.7 billion in 2050, with a peak of roughly 11 billion around 2100. More than half of the population of world already lives in urban areas, and this figure is expected to rise to 6.4 billion by 2050 (Population | United Nations, 2022).

The worldwide urban area is expanding at twice the pace of population increase, and it has been replacing vegetation-covered areas with impermeable ones that are dry in climate (Yao et al., 2017).

This has resulted in the emergence of "Urban heat islands effect" (UHI effect), where urban areas attain higher temperatures than their surrounding regions (Dhir, 2021). Such heat islands have far-reaching consequences for urban areas, chief among them a rise in the cost of maintaining a comfortable living and working environment (Zeng, 2021). The reduction of natural vegetation cover is one of the major issues brought on by urbanization. In terrestrial ecosystems, vegetation plays a significant role and has several advantages for human culture. Even the earth's lungs have been compared to the forest (MacLachlan et al., 2021). In addition to reducing the effects of air, noise, and urban heat islands, vegetation also prevents soil and water loss by retaining precipitation and reduces the greenhouse impact by absorbing CO_2. However, a number of the advantages of vegetation are also being reduced as a result of urbanization. For instance, urbanization has been converting cropland and forest into built-up areas, directly lowering the amount of vegetation (Yao et al., 2017). Changes in vegetation cover have a significant impact on ecosystem services, affecting ecosystem functioning from the local to the global scales as well as human variables such as the environment and policy planning (Sahana et al., 2016a). In naturally vegetated regions, plants absorb moisture from the soil and store it all in their leaves and stems. Transpiration causes this water to finally be discharged into the atmosphere. This process helps the plants cool both themselves and their surroundings. In urban areas, buildings, sidewalks, parking lots, and highways mostly are replacing plantations and other natural greenery (Gui et al., 2019). which causes, vegetation areas are reducing in these urban areas, there is significantly less transpiration, which eventually results in less cooling air of the environment. Elevated temperatures result from materials used in urban construction, including cement, asphalt, brick, glass, and steel, absorbing and storing more heat that is then reflected back into the environment (Sood & Patil, 2021). These materials are impermeable, unlike natural surfaces, so water cannot travel across them and eventually collapse into the soil. These surfaces have no way to stay cold without a cycle of water flowing and evaporating (Kandya & Mohan, 2018).

The Normalized difference vegetation index (NDVI) has a strong capacity to communicate across yearly and seasonal fluctuation in the activity of the vegetation cover and vegetation's responsiveness to climate change. The NDVI values have related to the biological activities of vegetation, and changes in the NDVI values indicate the various biochemical processes of vegetation (Yang et al., 2020). The daily changes in LST may be adequately described by the NDVI statistics, which represents the condition of vegetative cover. The NDVI may also be used to examine various vegetative microclimatic cycles at the local and global levels (Ruiz-Aviles et al., 2020). The NDVI may be used to monitor the health of natural vegetation, the susceptibility of vegetation to climate changes, and seasonal biological processes. The growth and development stages of vegetation cover may be tracked using NDVI. The NDVI values are determined by maximum near-infrared reflectance and maximum red reflectance (Grover & Singh, 2015). Since vegetation cover productivity is connected to evapotranspiration and precipitation, NDVI is a useful approach for analyzing vegetation cover efficacy at the landscape scale (Karimi et al., 2022). Remote Sensing (RS) and Geographic information system (GIS) have demonstrated to be particularly useful in evaluating and analyzing multi-temporal NDVI as well as UHI/LST. RS satellite image-based multitemporal NDVI data has taken at a certain time and place. The RS and GIS have a great capacity to map and examine NDVI and LST variations (Jain et al., 2020). In recent decades, research projects have significantly depended on satellite remote sensing spatial data for mapping specific vegetation cover and analyzing diversity in vegetation patterns. (Rani et al., 2018).

The major objectives of this study are:

1) To examine multi-temporal UHI/LST and NDVI in the Patna Municipal Corporation (PMC) from 1990 to 2022 using remotely sensed data and GIS.
2) To analyze the impact, determine the multi-temporal land surface temperature LST/UHI and NDVI across time (PMC).
3) To examine the average growth in UHI/LST in PMC between 1990 and 2022.
4) To examine the correlation between UHI/LST, and NDVI in PMC.

II. MATERIAL AND METHODS

A. *Study Area*

Patna, the capital of Bihar, is the fifth-fastest growing city in India, and 21st rapidly growing city in the world. It is expected to rise by 3.72% year on average.(Economy | District Patna, Government of Bihar | India, 2022). The Patna Municipal Corporation (PMC), which is situated on the Ganges River's southern bank, can be found between the latitudes of 25°33'10" and 25°39'03" north and 85°03'16" and 85°16'10" east (Ahmad & Munim, 2020). PMC is the epicenter of Commerce and trade in Bihar.

Source: File: Bihar district location map Patna.svg - Wikimedia Commons

Fig.2.1 Layout map of Bihar state, India

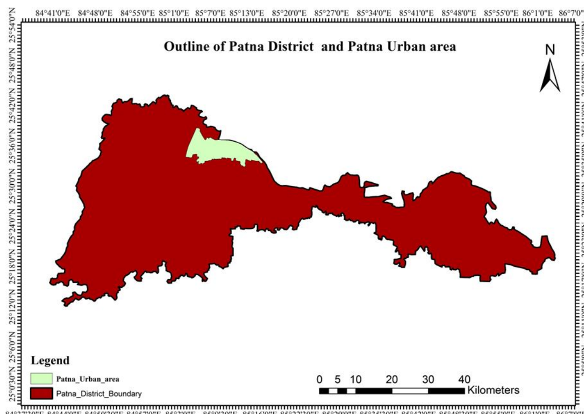

Fig.2.2 Layout map Patna district and PMC

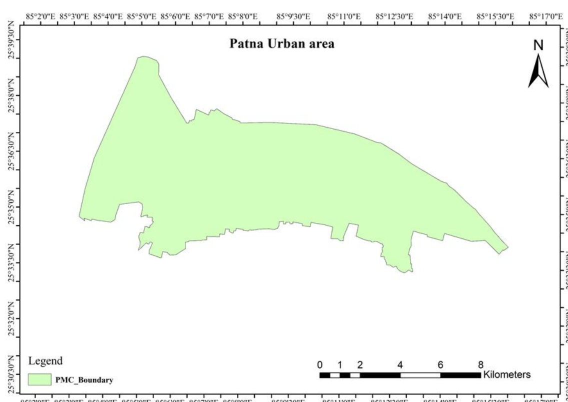

Fig.2.3 Layout map of PMC

The majority of the city's commercial establishments are located along the arterial and major roads, and there is subtantial commercial and residential land use throughout the city (Debjani Sarkar, 2015). Patna Municipal Corporation (PMC) covers nearly 100.8 square kilometers, as shown in Fig.2.3 (PMC's base map is based on the same map data used by Bihar Urban Development Infrastructure Development Corporation Ltd. (BUIDCO) for its National Mission for Clean Ganga (NMCG) project.) And it was divided into six circles and 72 wards (Annexure 12, BUIDCO, 2014).

International Journal for Research in Applied Science & Engineering Technology (IJRASET)
ISSN: 2321-9653; IC Value: 45.98; SJ Impact Factor: 7.538
Volume 11 Issue I Jan 2023- Available at www.ijraset.com

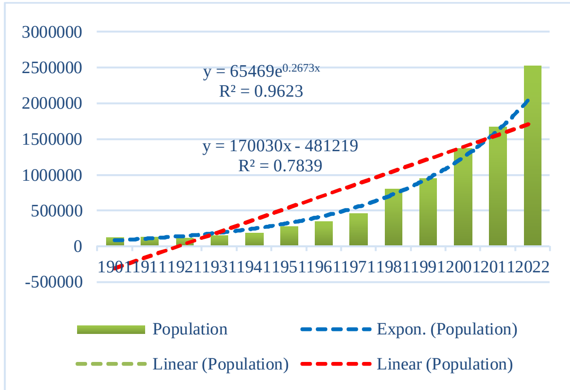

Fig.2.4 Population growth in PMC (1901-2022)

According to the Census of India (up to 2011), and United Nations, the city has a total population of 25,29,000 people, and the population density is 23,229 people per square kilometer. Between 1951 and 2022, population growth has generally shown on increasing trends. From 1961 to 2022, there is an exponential population growth (R^2 = 0.9884) trend shown in Fig.2.4 (World Population Dashboard, 2022). According to the findings of the previous study, the PMC has been expanding toward the west (Bihta and Danapur), while the older portion of the city on the east side, has overcrowding issues, which have put a significant strain on the city's physical infrastructure and caused traffic congestion. The central and western regions of the study area contain the more recently developed areas according to urban planning (Ashraf, 2015). PMC, lying in the tropical region experiences composite climate. The weather in PMC, summers are hot and humid, with temperatures ranging from 37.78°C to 44.45°C. The weather is pleasant throughout the monsoon season, and it is mild in the fall. Winters are mild, with temperatures in January ranging from 10-15.5°C. The average annual Rainfall 1,143 mm (Patna Municipal Corporation, 2022).

B. Methodology

The spatiotemporal patterns of LST in Patna Municipal Corporation has examined and compared to the NDVI and LULC pattern of vegetative condition. The researchers have made great strides, which has encouraged the use of remote sensing data in larger discussions about how fluctuations in LST and NDVI affect people's health and the urban environment (Sahana et al., 2016). Remote Sensing data and GIS application have been used to examine multi-temporal NDVI and LST in the Patna Municipal Corporation (PMC) from 1990 to 2022. The availability of high resolution, repeating coverage, and the capacity to monitor the conditions of the earth's surface are all advantages of using remote sensing data (Cao et al., 2022). The source of data is taken from journal papers, books, policy & reports.

1) Landsat Imagery Data

Landsat satellite image tiles (Landsat-5 Thematic Mapper (TM) and Landsat-8 Thermal Infrared Sensor (TIRS)) of 30 m pixel size covering the study area with cloud coverage of less than 10% of the same season in the early month of March for the maximum accuracy (Chettry & Surawar, 2021) were collected from the website of the United States Geological Survey's (USGS), https://earthexplorer.usgs.gov, for the years 1990, 2001, 2011, and 2022 in order to determine the multi-temporal NDVI and UHI/LST in PMC. Table No. 1 contains a description of the Landsat satellite images' technical specifications.

Table No.1 Specification of Landsat imagery data

No.	Satellite / Sensors	Date	Pixel size	Band used	P / R
1	Landsat-5 / TM	08/03/1990	30 m	1 to 7	141/42
2	Landsat-5 / TM	06/03/2001	30 m	1 to 7	141/42
3	Landsat-5 / TM	02/03/2011	30 m	1 to 7	141/42
4	Landsat-8 / TIRS	16/03/2022	30 m	1 to 7 & 10	141/42

Fig.2.5 Follow chart of study methodology

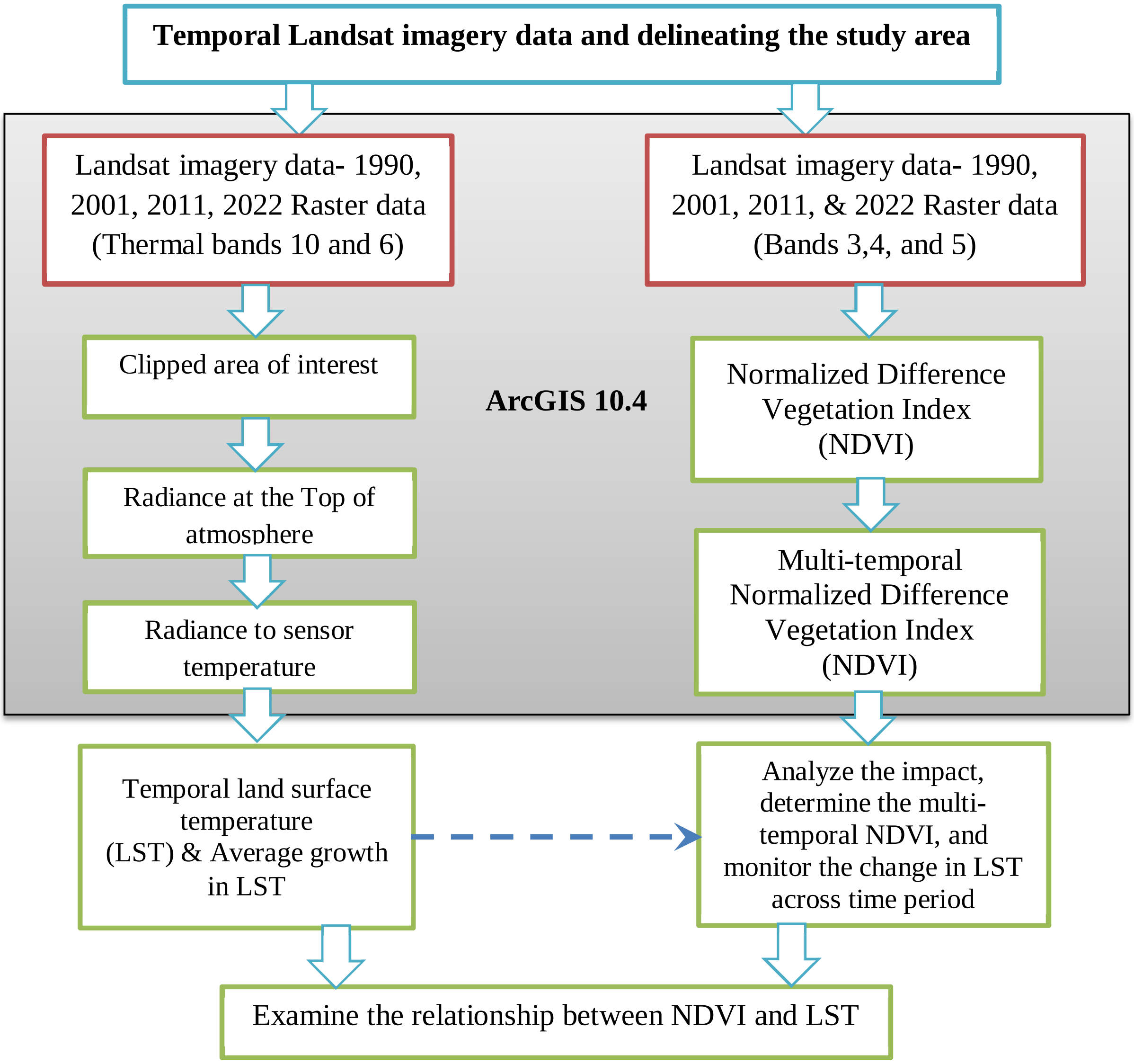

2) LST Extraction from Landsat Satellite images

The LST is an umbrella term that describes the average temperature of all terrestrial objects. Diverse researchers estimated the LST using Landsat data and defined measurements (Sahana et al., 2016). The LST values have been estimated using Landsat satellite images thermal band data (band 6 and band 10) (Puppala & Singh, 2021). All LST calculation steps are listed below as per follow chart of methodology fig.2.5.

Step 1: The top of the atmosphere (TOA) radiance is estimated using the digital numbers of the thermal infrared bands using the following formulae:

(a) For Landsat-5 / TM.

$$L\lambda = \frac{(LMAX - LMIN)}{(QCALMAX - QCALMIN) * (QCAL - QCALMIN) + LMIN}$$

where Lλ is the spectral radiance, QCAL is the digital number, LMIN is the spectral radiance that scales to QCALMIN, LMAX is the spectral radiance that scales to QCALMAX, QCALMIN is the minimum quantized calibrated pixel value (generally 1), and QCALMAX is the maximum quantized calibrated pixel value (typically 255)(Kikon et al., 2016).

(b) For Landsat-8 / TIRS

$$\mathbf{L\lambda = M_L \times Q_{cal} + A_L}$$

Where Lλ is the TOA spectral radiance in Watts / (m2× srad × μm), and M_L is the band-specific multiplicative rescaling factor (which is obtained from the metadata of the satellite imagery). AL is the additive rescaling factor that is band-specific (from the metadata of the satellite imagery). The quantized and calibrated standard product pixel values are denoted by Qcal (Kikon et al., 2016; Rani et al., 2018).

Step 2: The spectral radiance was changed into the sensor temperature in Kelvin by applying the following formula:

$$\mathbf{BT\ (K)} = \frac{K_2}{\ln\left(\frac{K_1}{L}\right)+1}$$

where K1 and K2 are the thermal conversion constants for the band 10, 6 of the thermal spectrums, which are derived from the metadata of the satellite image (Mushore et al., 2022).

Step 3: The final step is to calculate LST using the sensor temperature (BT), Conversion of Kelvin to Celsius (Ashraf, 2015), LST can be obtained using the following formula:

$$\mathbf{LST\ (°C) = BT\ (K) - 273.15}$$

C. NDVI Estimation

The Normalized Difference Vegetation Index (NDVI), a dimensionless index used to determine how much vegetation is present in a given area of land, analyzes the difference in vegetation cover between visible and near-infrared reflectance. The NDVI is determined by dividing the difference in near-infrared (NIR) and red (RED) reflectance by the total of these two values. where the near-infrared (NIR) and red reflectance (RED) are represented by bands 5 and 4 of the Landsat-8 and bands 4 and 3 of the Landsat-5 satellite images, respectively. Additionally, the NDVI calculated from Landsat images has characteristic values between - 1 and + 1. Higher NDVI values indicate more green vegetation density, whereas lower values indicate moisture-stressed vegetation (Rashid et al., 2022). The NDVI-based land type classification with NDVI value is shown in Table No.2 (Puppala & Singh, 2021).

$$\mathbf{NDVI} = \frac{(\mathrm{NIR-RED})}{(\mathrm{NIR+RED})}$$

III. RESULTS AND DISCUSSIONS

A. Multi-Temporal UHI/LST Pattern Analysis

(Fig.3.1 to Fig.3.4) show the areal pattern of LST in PMC for the base years 1990, 2001, 2007, and 2022 with light to dark brown shades indicating warmer locations and light to deep green coolers indicating colder locations in the study area. The geographic patterns of LST are temporal and concentration altering. The LST of PMC has increased due to rapid NDVI changes. The LST was estimated to be in the range of 17.3–24.5 °C during 1990, 20.2–31.6 °C during 2001, 19.7–30.8 °C during 2011, and 24.2–33.5 °C during 2022.

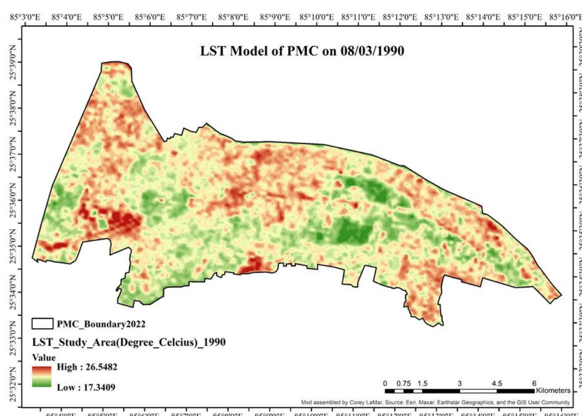

Fig. 3.1 LST model of PMC on 08/03/1990

International Journal for Research in Applied Science & Engineering Technology (IJRASET)
ISSN: 2321-9653; IC Value: 45.98; SJ Impact Factor: 7.538
Volume 11 Issue I Jan 2023- Available at www.ijraset.com

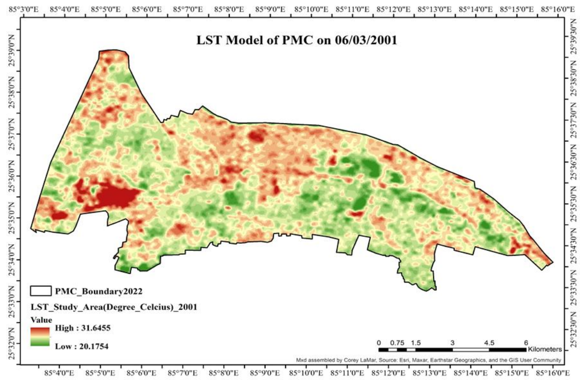

Fig. 3.2 LST model of PMC on 06/03/2001

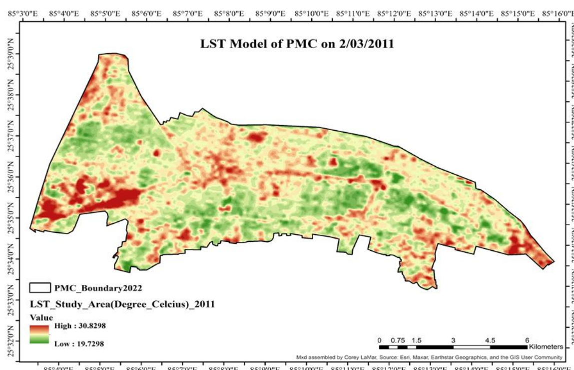

Fig. 3.3 LST model of PMC on 02/03/2011

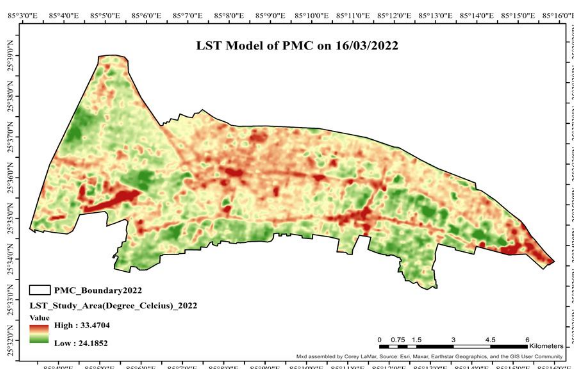

Fig. 3.4 LST model of PMC on 16/03/2022

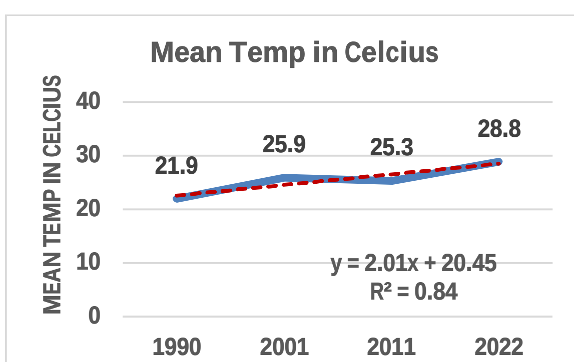

Graph- 3A Mean LST over the period

This increase is purely mathematical; however, more accurate temperature growth estimates have been made using the geographic average, and they reveal that between 1990 and 2022, the mean UHI/LST has risen by around 6.88 °C (the linear regression analysis is displayed in Graph-3A). For this modification, R^2 = 0.84). The UHI/LST has increased due to the increased build-up in the study area from 1990 to 2022. The built-up area has covered with roads, flyovers, buildings, concrete structure and other impermeable surfaces, which because of their greater thermal conductivity absorb more solar energy during the day and release it gradually as emissions at night. As a result, compared to nearby rural regions, urban areas often have greater temperatures. Urban growth, often to responsible for the dramatic rise in earth's surface temperature because vegetation cover has been replaced with non-evaporating and non-transpiring shells made of metal, asphalt, and concrete. Due to more vegetation and open agricultural land, the study area's southern, eastern, and western areas experience lower temperatures. In contrast, the central zone and airport area have recorded increased LST as a result of growing urbanization, dwindling waterbodies and vegetation. The greatest variance was seen in the maximum and lowest temperatures for the years 2022 (33.5 °C and 24.2 °C, respectively). The highest and lowest temperature differences in 1990 were 24.5 and 17.3 degrees Celsius, respectively. Taking all of the restrictions of Remote Sensing-derived UHI/LST estimation into consideration, the variance between estimated and recorded LST is acceptable and may be used for further analysis, such as UHI/LST simulation and temperature, condition index in the study area. Furthermore, the highest LST values in PMC were calculated in the city's core region, which is densely populated and rapidly increasing, indicating a positive interaction between LST and built-up zones and a negative correlation with NDVI. Therefore, while developing urbanization, the environmental impact must be taken into account.

B. *Multi-temporal NDVI Pattern Analysis*

The spectral properties of vegetation, which absorbs visible light, energy required in photosynthesis, and reflects near-infrared (NIR) radiation, are used to calculate NDVI using Landsat imagery. (Fig.3.5 to Fig.3.12) show the NDVI models and their values of Histogram have developed from Landsat satellite data from 1990, 2001, 2011, and 2022. The vegetation cover has been identified using the ArcGIS Pro software. The NDVI values in the study area ranged from -0.32 to +0.67 in 1990, -0.26 to +0.60 in 2001, and -0.19 to +0.64 in 2011. while NDVI values have changed, from -0.04 to +0.46 in 2022. Higher NDVI values indicated that places with thick vegetation and forests are the most productive. Lower NDVI values, on the other hand, indicated the presence of fewer and less productive zones, such as waterbodies, built-up areas, and barren terrain. Therefore, as per literature reviews, NDVI range values have been classified into typical land use types in the study area, which is shown in histogram graphs and Table No. 2.

Table No.2. NDVI-based land type classification

No.	NDVI Range		Types of land
1	-0.0	-0.015	Water Body
2	-0.15	0.14	Built-up area
3	0.14	0.18	Barren Land
4	0.18	0.27	Shrubs and Grassland
5	0.27	Up to +1	Dense Vegetation

According to this study, the NDVI models and their histogram has been showing the frequency of land cover shifted to the built-up area or nonproductive areas under the considered period. Overall, it has evident that between 1990 and 2022, the study area's biodiversity and vegetation cover significantly decreased. It has been reported that the (NDVI values) have changed significantly between 1990 and 2022. These are a consequence of an increase in built-up areas in the study area.

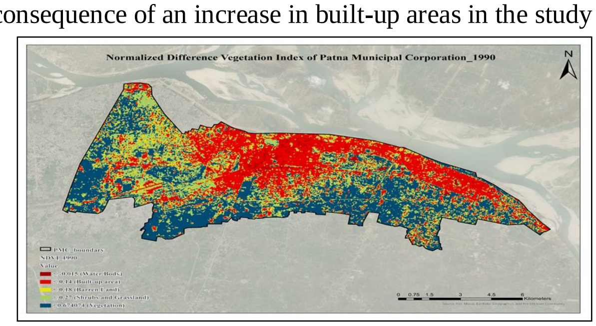

Fig. 3.5 NDVI Model of PMC (1990)

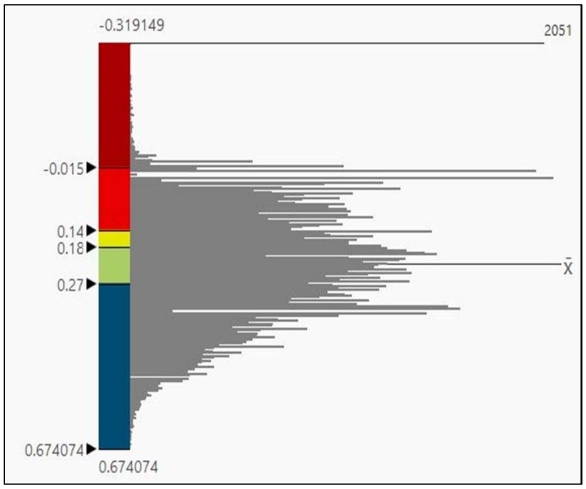

Fig. 3.6 Histogram of the Range of NDVI Values for land covers in PMC (1990)

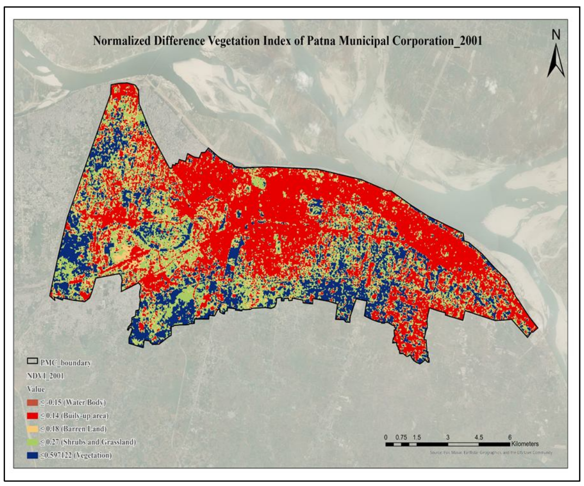

Fig. 3.7 NDVI Model of PMC (2001)

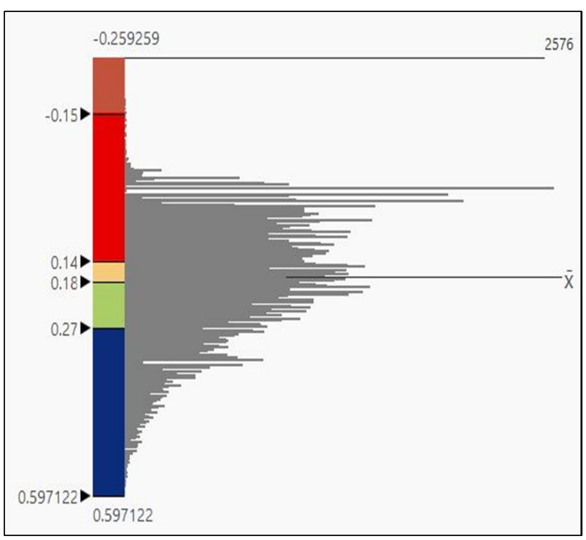

Fig. 3.8 Histogram of the Range of NDVI Values for land covers in PMC (2001)

ISSN: 2321-9653; IC Value: 45.98; SJ Impact Factor: 7.538
Volume 11 Issue I Jan 2023- Available at www.ijraset.com

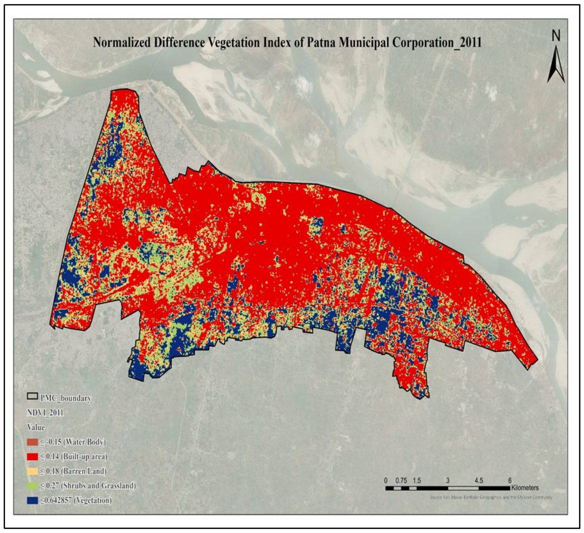

Fig. 3.9 NDVI Model of PMC (2011)

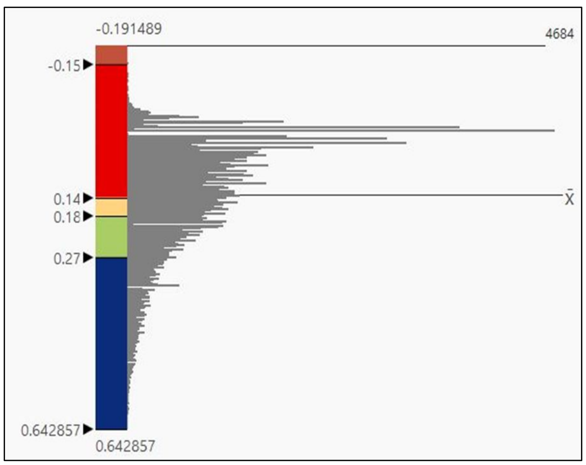

Fig. 3.10 Histogram of the Range of NDVI Values for land covers in PMC (2011)

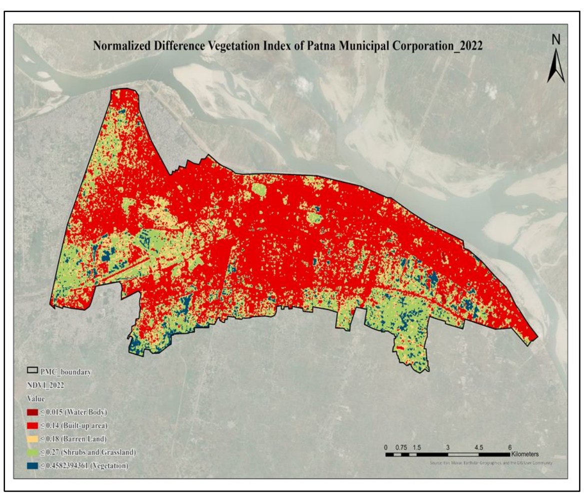

Fig. 3. 11 NDVI Model of PMC (2022)

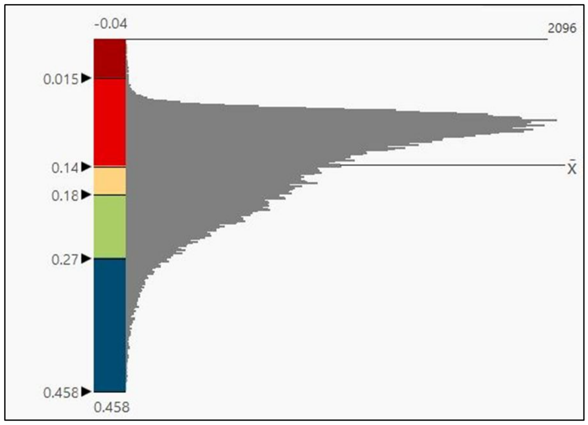

Fig. 3.12 Histogram of the Range of NDVI Values for land covers in PMC (2022)

On the other side, there has been a major rise in built-up areas on the southern and western sides of the municipal area of Patna. Many urban green spaces have been transformed into flyovers, roadways, residential colonies, and commercial centers. Along with the residential sector's densification, the commercial areas are expanding as well. The major topic of the present study is the NDVI of PMC. This vegetative component is important for the long-term growth of an urbanized city or municipal territory. In the early literature, the experiment of biological processes including photosynthesis, transpiration, respiration, and the distribution of dry weight basis among vegetative organs, as well as water permeability by roots and carbohydrate acceptance, has more concerned with the growth of vegetation (urban greens). The area covered by urban green spaces has typically represented an inversely proportionate relationship with the progress of urbanization in the Patna municipal corporation area. According to data study, the amount of vegetation has shrunk by more than one-third since 1990, which is particularly concerning for city planners since the loss in a city's productive area has a detrimental impact on the sustainability of the city.

C. Relationship Between LST, and NDVI

The term "NDVI" reflects the amount of radiation from plants that is actively engaged in photosynthetic processes. As a result, the NDVI value in the study area is strongly influenced by climatic factors, soil, and geomorphology. The graphs (Graph 3B to 3E) show the link with NDVI and UHI/LST. The regression line provided significant clarification, demonstrating a strong inverse link between UHI/LST and NDVI. The linear regression analysis (R2) for the analysis period revealed that UHI/LST and NDVI are inversely correlated, with R2 values of 0.93, 0.94, 0.92, and 0.77 for the years 1990, 2001, and 2022, respectively. These findings suggest that vegetation-covered areas have decreased as a result of urbanization, which has contributed in the effect of UHI/LST. The inverse relation between LST and NDVI demonstrates that the higher the amount of vegetation cover, the lower the LST. The NDVI has a significant influence on LULC fluctuations. It also means that the territories with the lowest NDVI values have less vegetative spread as a consequence of urban expansion, whereas higher NDVI values imply a dense vegetal spread, and LST rises as a result of the decrease in vegetal density. A strong relationship has been observed between UHI/LST and NDVI,

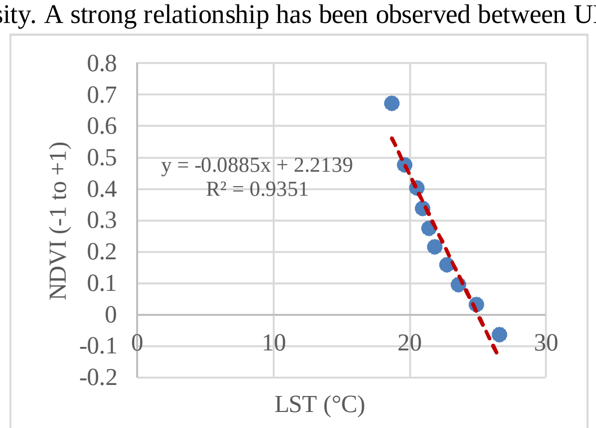

Graph- 3B LST and NDVI correlation for the year 1990

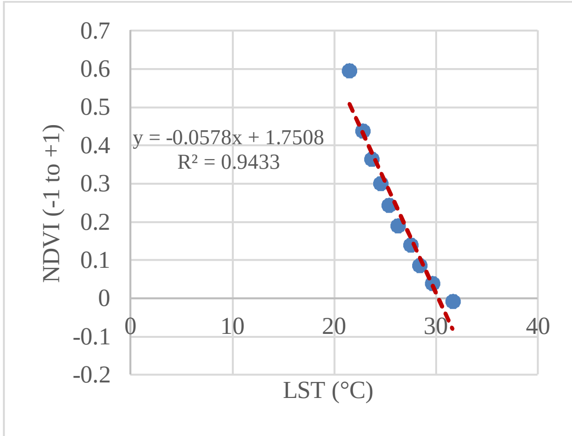

Graph- 3C LST and NDVI correlation for the year 2001

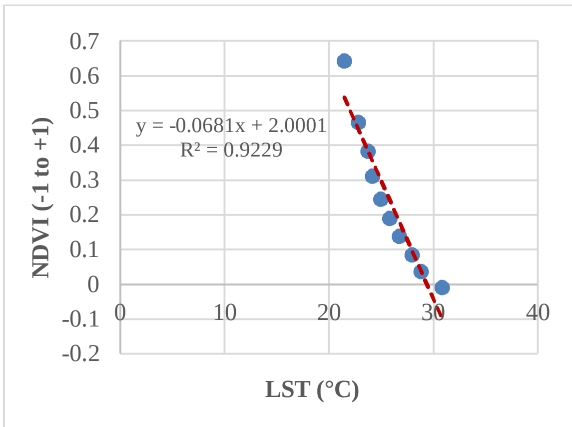

Graph- 3D LST and NDVI correlation for the year 2011

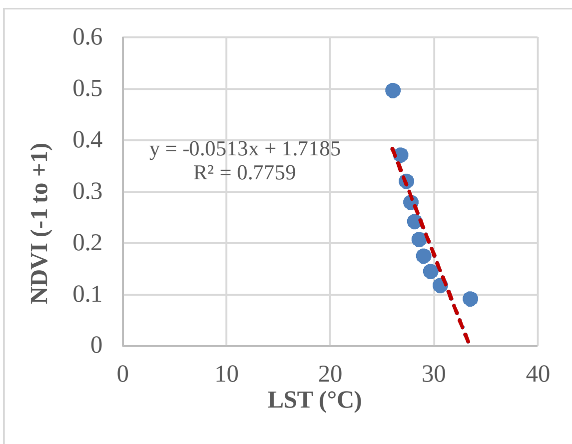

Graph- 3E LST and NDVI correlation for the year 2022

demonstrating that a direct regression may be used to predict UHI/LST provided NDVI values are known in the study area. In the future, the NDVI can be used to compute the LST precisely. The NDVI values are thought to have declined between 1990 and 2022 because to increased urbanization and decreased vegetation cover. The highest LST values show the lowest NDVI and vice versa. They also highlight the difference between places with high LST and those with low temperatures in terms of the amount of vegetation that is present in each location.

IV. CONCLUSION

The NDVI reflects the photosynthetically active radiation for vegetation. The NDVI value in PMC has greatly influenced by environmental factors such as soil and geomorphology. According to the regression analysis, there is a significant interaction effect between UHI/LST and NDVI. Our findings show that increases in UHI/LST have mostly caused by reductions in vegetative patches. These changes have resulted in the loss of natural ecology and biodiversity, and the expansion of built-up areas may be the root cause of other environmental problems. Rapid urbanization and a reduction in vegetation areas in cities are inversely correlated. Additionally, PMC has manifested an increase in mean LST that is greater than 6°C, which is sufficient for the UHI effect to emerge, because of the growing buildup areas. UHI/LST have a positive relationship with population growth, which contributes to urbanization, with more densely and highly urbanized areas having greater temperatures than urban vegetative areas. Understanding the process of land use, cover and the influence of LST/UHI are critical components of urban planning for urban planners and architects, allowing for more control over the surrounding environment. It was found that Patna's municipal corporation has been noticeably more prone to unfavorable land use, cover shift and heat island. An all-encompassing and integrated planning effort must be made in order to handle this growing issue.

A. Limitations

The limitations of this study include that all data was gathered from secondary sources, such as the USGS site, the Census of India, and the United Nations for the base years that have been utilized for accuracy evaluation.

B. Acknowledgements

The authors would like to thank the Faculties of the Department of Architecture and Planning at NIT Patna for their valuable comments, which helped in the improvement of this article. The authors would like to express their appreciation to the USGS Earth Explorer for providing the satellite data available.

C. Conflict of Interest

The authors have acknowledged that they have no conflicts of interest.

REFERENCES

[1] Ahmad, M. Y., & Munim, N. H. (2020). Approach of Remote Sensing and GIS Techniques of Land Use and Land Cover Mapping –Patna Municipal Corporation, (PMC) Patna, Bihar, India. Current World Environment, 371–377. https://doi.org/10.12944/cwe.15.2.25

[2] Anindita Bhattacharjee. (2022). Urban Heat Island Effect_ A Case Study of Jaipur, India [#1018122]-2059777. Nternational Journal of Earth Sciences Knowledge and Applications, 4(1), 134–139. Annexure 12. (n.d.).

[3] Ashraf, M. (2015). A STUDY OF TEMPORAL CHANGE IN LAND SURFACE TEMPERATURE AND URBAN HEAT ISLAND EFFECT IN PATNA MUNICIPAL CORPORATION OVER A PERIOD OF 25 YEARS (1989-2014) USING REMOTE SENSING AND GIS TECHNIQUE. International Journal of Remote Sensing & Geoscience (IJRSG), 4(1). www.ijrsg.com

[4] Cao, L., Li, P., Zhang, L., & Chen, T. (n.d.). REMOTE SENSING IMAGE-BASED ANALYSIS OF THE RELATIONSHIP BETWEEN URBAN HEAT ISLAND AND VEGETATION FRACTION.

[5] Chettry, V., & Surawar, M. (2021). Assessment of urban sprawl characteristics in Indian cities using remote sensing: case studies of Patna, Ranchi, and Srinagar. Environment, Development and Sustainability, 23(8), 11913–11935. https://doi.org/10.1007/s10668-020-01149-3

[6] Debjani Sarkar, G. (1989). An Assessment of Declining Urban Greens under Patna Municipal Corporation Based on Normalized Difference Vegetation Index *1. www.environmentaljournal.org

[7] Dhir, A. (2021). Evaluation of Urban Heat Island Effect in Cybercity, New Delhi Using a 3D Urban Microclimate Model: Envi-Met Item Type text; Electronic Thesis. http://hdl.handle.net/10150/660139

[8] Economy | District Patna, Government of Bihar | India. (n.d.). Retrieved January 15, 2023, from https://patna.nic.in/economy/

[9] Grover, A., & Singh, R. B. (2015). Analysis of urban heat island (Uhi) in relation to normalized difference vegetation index (ndvi): A comparative study of delhi and mumbai. Environments - MDPI, 2(2), 125–138. https://doi.org/10.3390/environments2020125

[10] Gui, X., Wang, L., Yao, R., Yu, D., & Li, C. (2019). Investigating the urbanization process and its impact on vegetation change and urban heat island in Wuhan, China. Environmental Science and Pollution Research, 26(30), 30808–30825. https://doi.org/10.1007/s11356-019-06273-w

[11] Jain, S., Sannigrahi, S., Sen, S., Bhatt, S., Chakraborti, S., & Rahmat, S. (2020). Urban heat island intensity and its mitigation strategies in the fast-growing urban area. Journal of Urban Management, 9(1), 54–66. https://doi.org/10.1016/j.jum.2019.09.004

[12] Kandya, A., & Mohan, M. (2018). Mitigating the Urban Heat Island effect through building envelope modifications. Energy and Buildings, 164, 266–277. https://doi.org/10.1016/j.enbuild.2018.01.014

[13] Karimi, A., Mohammad, P., García-Martínez, A., Moreno-Rangel, D., Gachkar, D., & Gachkar, S. (2022). New developments and future challenges in reducing and controlling heat island effect in urban areas. In Environment, Development and Sustainability. Springer Science and Business Media B.V. https://doi.org/10.1007/s10668-022-02530-0

[14] Kikon, N., Singh, P., Singh, S. K., & Vyas, A. (2016). Assessment of urban heat islands (UHI) of Noida City, India using multi-temporal satellite data. Sustainable Cities and Society, 22, 19–28. https://doi.org/10.1016/j.scs.2016.01.005

[15] MacLachlan, A., Biggs, E., Roberts, G., & Boruff, B. (2021). Sustainable City Planning: A Data-Driven Approach for Mitigating Urban Heat. Frontiers in Built Environment, 6. https://doi.org/10.3389/fbuil.2020.519599

[16] Marando, F., Heris, M. P., Zulian, G., Udías, A., Mentaschi, L., Chrysoulakis, N., Parastatidis, D., & Maes, J. (2022). Urban heat island mitigation by green infrastructure in European Functional Urban Areas. Sustainable Cities and Society, 77. https://doi.org/10.1016/j.scs.2021.103564

[17] Mushore, T. D., Mutanga, O., & Odindi, J. (2022). Determining the Influence of Long-Term Urban Growth on Surface Urban Heat Islands Using Local Climate Zones and Intensity Analysis Techniques. Remote Sensing, 14(9). https://doi.org/10.3390/rs14092060

[18] Patna Municipal Corporation. (n.d.). Retrieved January 15, 2023, from https://www.pmc.bihar.gov.in/weather.aspx

[19] Population | United Nations. (n.d.). Retrieved January 14, 2023, from https://www.un.org/en/global-issues/population

[20] Puppala, H., & Singh, A. P. (2021). Analysis of urban heat island effect in Visakhapatnam, India, using multi-temporal satellite imagery: causes and possible remedies. Environment, Development and Sustainability, 23(8), 11475–11493. https://doi.org/10.1007/s10668-020-01122-0

[21] Rani, M., Kumar, P., Pandey, P. C., Srivastava, P. K., Chaudhary, B. S., Tomar, V., & Mandal, V. P. (2018). Multi-temporal NDVI and surface temperature analysis for Urban Heat Island inbuilt surrounding of sub-humid region: A case study of two geographical regions. Remote Sensing Applications: Society and Environment, 10, 163–172. https://doi.org/10.1016/j.rsase.2018.03.007

[22] Rashid, N., Alam, J. A. M. M., Chowdhury, M. A., & Islam, S. L. U. (2022). Impact of landuse change and urbanization on urban heat island effect in Narayanganj city, Bangladesh: A remote sensing-based estimation. Environmental Challenges, 8. https://doi.org/10.1016/j.envc.2022.100571

[23] Ruiz-Aviles, V., Brazel, A., Davis, J. M., & Pijawka, D. (2020). Mitigation of Urban Heat Island Effects through “Green Infrastructure”: Integrated Design of Constructed Wetlands and Neighborhood Development. Urban Science, 4(4), 78. https://doi.org/10.3390/urbansci4040078

[24] Sahana, M., Ahmed, R., & Sajjad, H. (2016a). Analyzing land surface temperature distribution in response to land use/land cover change using split window algorithm and spectral radiance model in Sundarban Biosphere Reserve, India. Modeling Earth Systems and Environment, 2(2). https://doi.org/10.1007/s40808-016-0135-5

[25] Sahana, M., Ahmed, R., & Sajjad, H. (2016b). Analyzing land surface temperature distribution in response to land use/land cover change using split window algorithm and spectral radiance model in Sundarban Biosphere Reserve, India. Modeling Earth Systems and Environment, 2(2). https://doi.org/10.1007/s40808-016-0135-5

[26] Sood, R., & Patil, A. S. (2021). MITIGATION OF URBAN HEAT ISLAND EFFECT THROUGH DESIGN.

[27] World Population Dashboard. (n.d.). Retrieved January 15, 2023, from https://www.unfpa.org/data/world-population-dashboard

[28] Yang, Z., Witharana, C., Hurd, J., Wang, K., Hao, R., & Tong, S. (2020). Using Landsat 8 data to compare percent impervious surface area and normalized difference vegetation index as indicators of urban heat island effects in Connecticut, USA. Environmental Earth Sciences, 79(18). https://doi.org/10.1007/s12665-020-09159-0

[29] Yao, R., Wang, L., Gui, X., Zheng, Y., Zhang, H., & Huang, X. (2017). Urbanization effects on vegetation and surface urban heat islands in China’s Yangtze River Basin. Remote Sensing, 9(6). https://doi.org/10.3390/rs9060540

[30] Zeng, Z. (2021). The impact of vegetation change and climate in coastal cities on public sports: the impact of urban heat island. Arabian Journal of Geosciences (2021). https://doi.org/10.1007/s12517-021-07199-9/Published

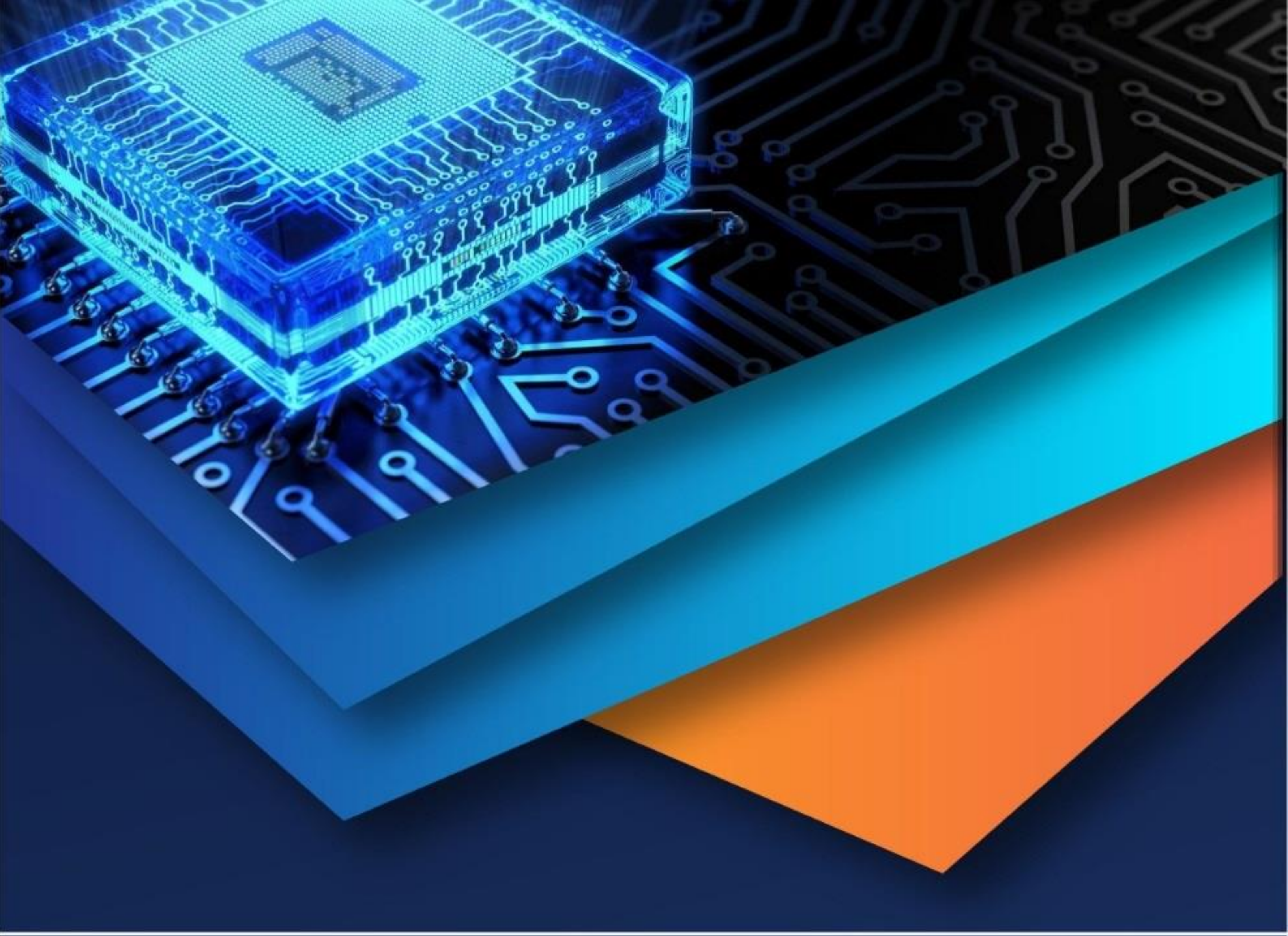

10.22214/IJRASET

INDEX COPERNICUS 45.98

ISRA JIF IMPACT FACTOR: 7.129

SJIFactor IMPACT FACTOR: 7.429

TOGETHER WE REACH THE GOAL

ISI

INTERNATIONAL JOURNAL FOR RESEARCH

IN APPLIED SCIENCE & ENGINEERING TECHNOLOGY